SMPL-A: Modeling Person-Specific Deformable Anatomy (Supplementary Material)

Hengtao Guo[1,2], Benjamin Planche[1], Meng Zheng[1], Srikrishna Karanam[1], Terrence Chen[1], Ziyan Wu[1]
[1]United Imaging Intelligence, Cambridge MA, USA
[2]Rensselaer Polytechnic Institute, Troy NY, USA
{first.last}@uii-ai.com, guoh9@rpi.edu

In this supplementary material, we provide further implementation details for reproducibility, as well as additional qualitative and quantitative results, covering different organs and highlighting the accuracy of our method. Finally, we share some insight w.r.t. real-world applications of our solution.

A. Implementation Details

Figure S2 serves as an supplement to the Section 4.2 in the main text. We use the Elastix registration [2] implemented in Slicer [1] to non-rigidly align the template mesh $\hat{M}$ to any given mesh M_k. After homogenizing the representation of the organ meshes, every organ mesh shall have exactly the same number of vertices, and vertices with the same index shall also point to corresponding anatomical structures, as in Figure S1.

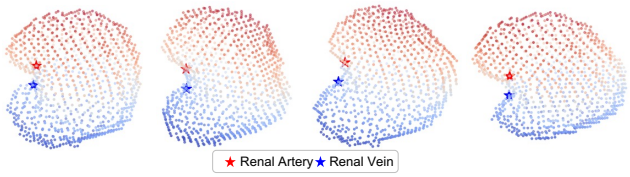

Figure S1. Corresponding landmarks, *i.e.*, the renal artery and renal vein, for left kidneys.

B. Additional Results

B.1. Multi-organ Results

As a supplement to the results of the left lung and spleen provided in the main text, we present the SMPL-A deformation prediction for the right lung (Figure S3), left kidney (Figure S4) and right kidney (Figure S5), follow the similar pattern as in Figure 7 in the main text.

For each subfigure (A), we show one deformation sequence, from rest pose to extreme pose, with the resulting organ prediction from SMPL-A compared to the baseline one. Since the baseline method is simply the mean shape of that particular sequence, the surface error mainly comes from the organ stretching on the upper/lower edges (caused by the FEM's nodal loads and surface constraints). By observing the error color coding, we can see that the SMPL-A's results have a much lower surface error, which indicates its capability of recovering the patient-specific organ's shape as well as the simulated deformation caused by the pose change (lifting the arms).

For each subfigure (B), we show how the SMPL-A's prediction changes according to the organ shape parameters α and pose parameters θ, respectively. The color map was encoded by the predicted stretching amount w.r.t. to the first frame inside one sequence. With changes in α, the recovered points cloud shows different organ shapes across patients; whereas with changes in θ, the predicted stretching amount gradually increases from the first row to the last row. This, again, suggests that the SMPL-A model learns (1) the patient-specific organ shape information and (2) the correspondence between the changes in organ's shape and human pose parameters.

B.2. Study of Organ Parameter α

In Figure S6, we demonstrate the necessity of introducing α in modeling the shape of organs. With the proposed additional information from α (SMPL-A in the second column), the recovered shapes have a high correspondence to the ground-truth. In comparison, we trained another decoder D' which directly predicts the organ's points cloud merely based on the SMPL's pose parameters θ and shape parameters β, *i.e.*, merely based on human external appearance. The resulting recovered organ shapes (third column) show a low variance from one patient to the other, and are very similar to the mean shape of that specific organ (fourth column). This suggests that to accurately estimate the organ shape deformation, it is necessary to combine both the internal and external information.

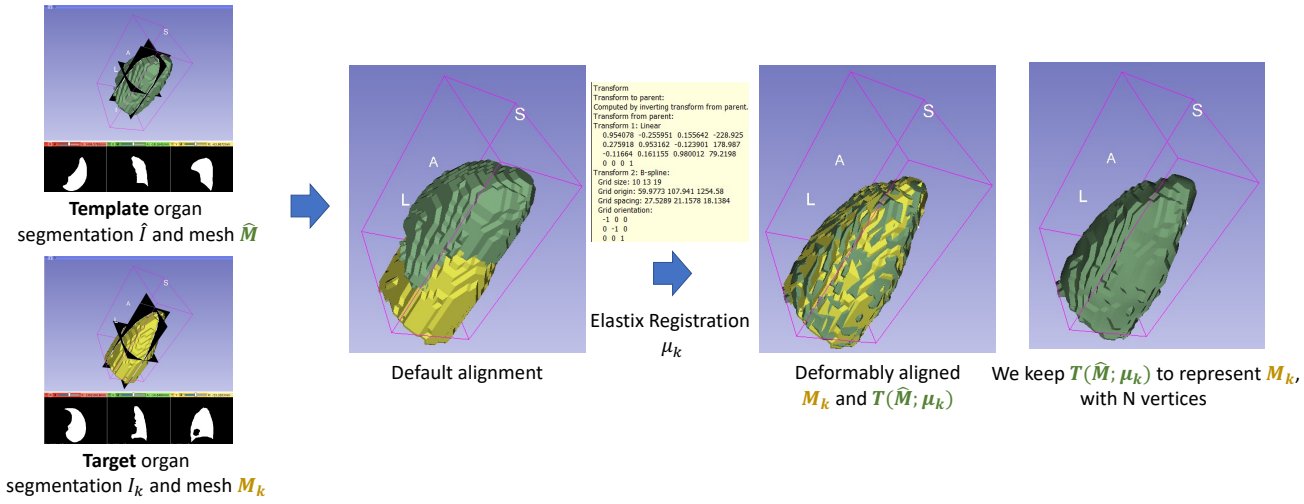

Figure S2. Organ registration. We use Elastix registration to homogenize the representation (number of vertices) for the same organ across different subjects.

C. Illustration of Real-life Applications

Our work targets a variety of medical use-cases (*cf*. Section 1 of the main paper). One of these applications is illustrated in Figures S7 and S8 (also in animated GIF files attached to this supplement). Given a patient's medical image information obtained from previous scans, we can use the SMPL-A encoder to extract and save the representation α of the patient's target organ(s). After a period of time, *e.g*., when the patient comes back to the hospital for a follow-up study, the patient's vector α can be passed to the SMPL-A decoder to estimate the patient's current organ deformation and warp the historical medical image correspondingly. This way, if new scans are captured during the present session, they can be directly compared to the warped historical scans, *e.g*., regardless of changes in the patient's pose during the present scanning procedure. By enabling such a direct one-to-one comparison of medical scans across time and poses, the clinicians could more easily perform their analysis, *e.g*., they could further examine the disease progression or the effectiveness of treatment in an intuitive way.

References

[1] R. Kikinis, S. D. Pieper, and K. G. Vosburgh. 3d slicer: a platform for subject-specific image analysis, visualization, and clinical support. In *Intraoperative imaging and image-guided therapy*, pages 277–289. Springer, 2014. 1

[2] S. Klein, M. Staring, K. Murphy, M. A. Viergever, and J. P. Pluim. Elastix: a toolbox for intensity-based medical image registration. *IEEE transactions on medical imaging*, 29(1):196–205, 2009. 1

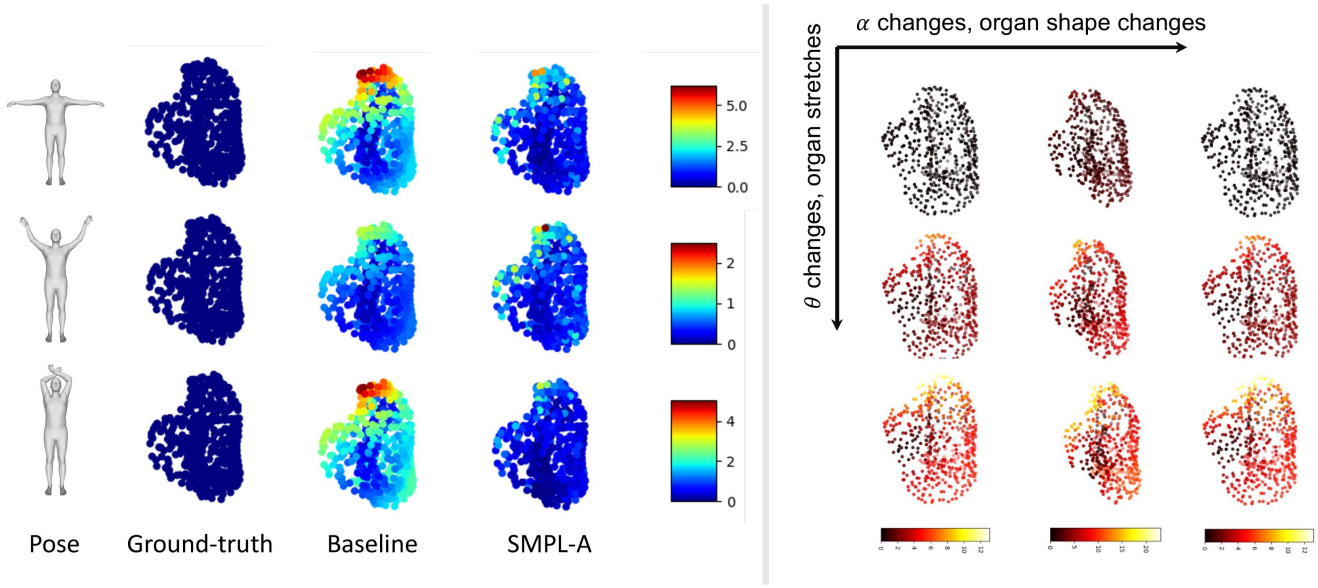

Figure S3. (A) Predicted deformation error (color-coded, in mm) for the right lung; (B) Impact of patients' pose parameter θ and organ parameter α on deformed right lung shape reconstruction (color-coded by the stretch amount w.r.t. the first frame in each sequence, in mm).

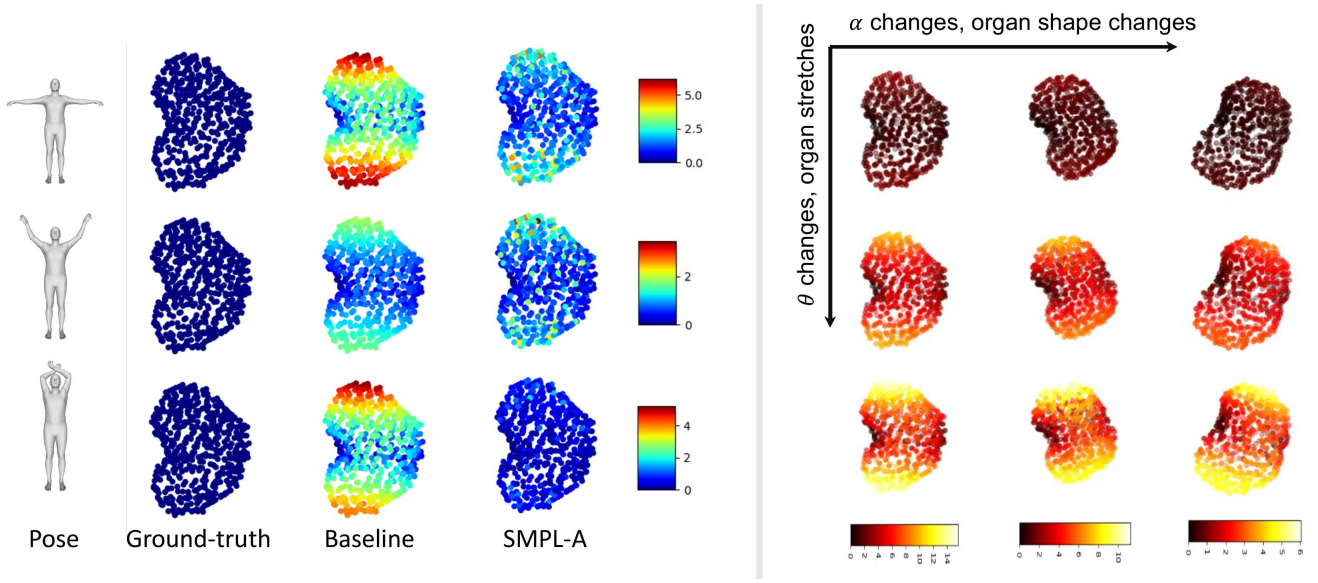

Figure S4. (A) Predicted deformation error (color-coded, in mm) for the left kidney; (B) Impact of patients' pose parameter θ and organ parameter α on deformed left kidney shape reconstruction (color-coded by the stretch amount w.r.t. the 1st frame in each sequence, in mm).

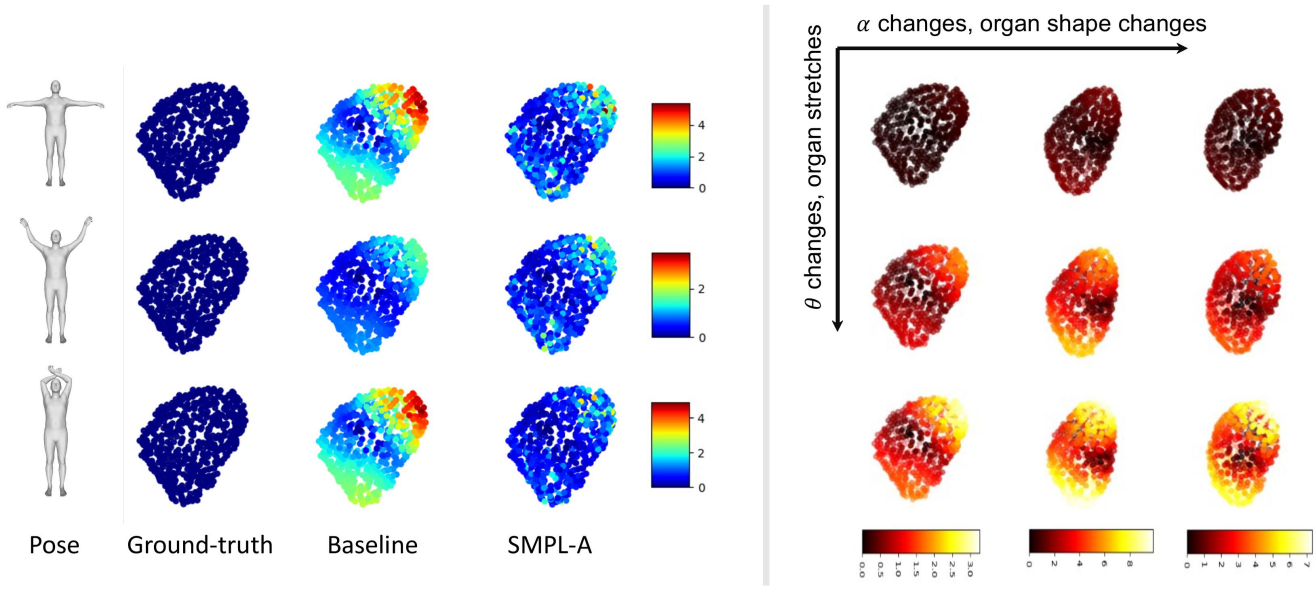

Figure S5. (A) Predicted deformation error (color-coded, in mm) for the right kidney; (B) Impact of patients' pose parameter θ and organ parameter α on deformed right kidney shape reconstruction (color-coded by the stretch amount w.r.t. the first frame in each sequence, in mm).

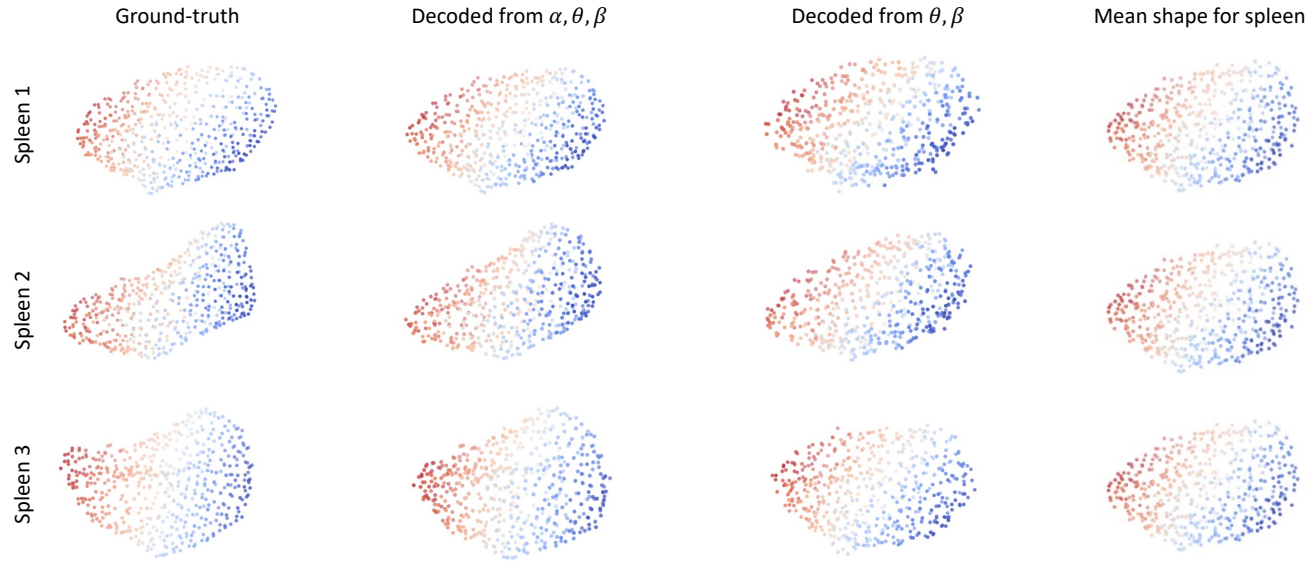

Figure S6. Importance of encoding patients' anatomical information. We show the necessity of α's information in accurate estimation of the patient-specific organ shape. The second column indicates our SMPL-A results; third column represents the results from a separately trained decoder D' which reconstructs organ shape merely depending on the θ and β, *i.e.*, merely based on the patient's external appearance; the fourth column shows the mean shape of spleen.

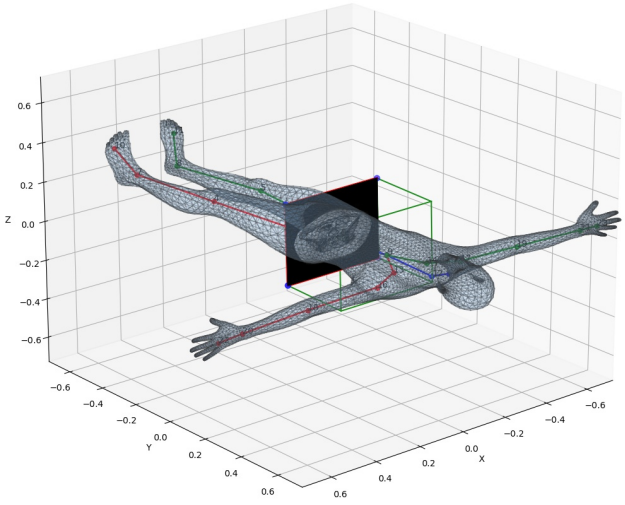

Figure S7. Demonstration. Sliding axial view of the MRI image (deformed by SMPL-A predictions) is overlaying with the patient's SMPL model. (To see the animation, please view the document with a compatible software, *e.g.*, *Adobe Acrobat* or *KDE Okular*; otherwise, the figure is also provided as a separate GIF file attached to the submission)

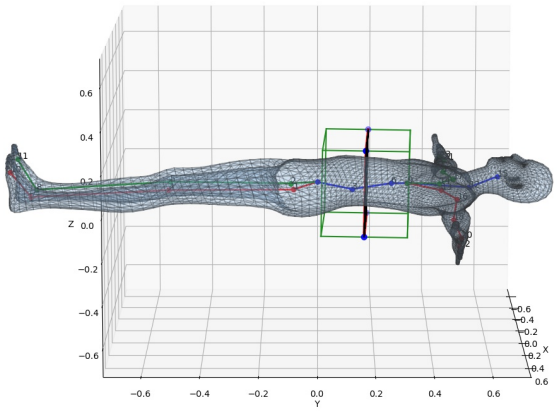

Figure S8. Demonstration. Circular round view of the MRI image (deformed by SMPL-A predictions) is overlaying with the patient's SMPL model. (To see the animation, please view the document with compatible software, *e.g.*, *Adobe Acrobat* or *KDE Okular*; otherwise, the animation is also provided as a separate GIF file attached to the submission)